Supplementary Materials for

Serum amyloid A delivers retinol to intestinal myeloid cells to promote adaptive immunity

Ye-Ji Bang, Zehan Hu, Yun Li, Sureka Gattu, Kelly A. Ruhn, Prithvi Raj, Joachim Herz, and Lora V. Hooper

correspondence to: lora.hooper@utsouthwestern.edu

This PDF file includes:

Figs. S1 to S17
Tables S1 to S3

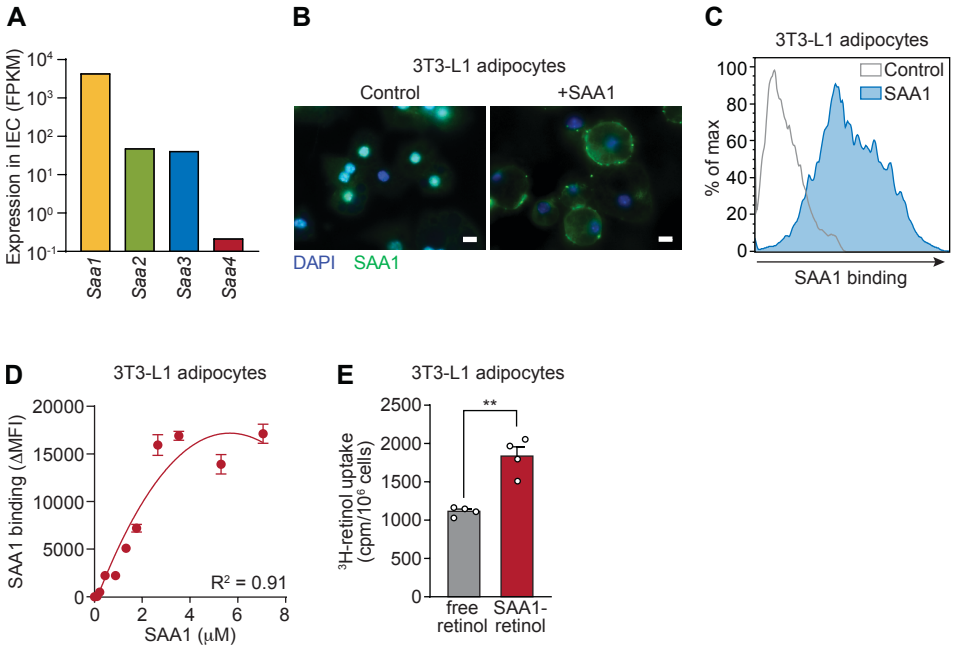

Fig. S1. 3T3-L1 adipocytes express cell-surface receptor(s) for SAA. (A) Expression of *Saa* transcripts in intestinal epithelial cells (IEC) was analyzed based on previously published RNA-sequencing data (*52*) (Gene Expression Omnibus accession number GSE134303). Data are from three pooled biological replicates of small intestinal epithelial cells acquired by laser capture microdissection (*52*). **(B, C)** Binding of SAA1 to the cell surface of 3T3-L1 adipocytes was analyzed by immunofluorescence assay (B) and flow cytometry (C). His-SAA1–retinol complexes were added to 3T3-L1 adipocytes and incubated for 1 hour at 4°C. **(B)** Cells were stained with Alexa Fluor 488-conjugated anti-His tag antibody to detect SAA (green) and nuclei were stained with DAPI (blue). Scale bars=10 μm. **(C)** SAA binding to the adipocyte cell surface was measured by flow cytometry. PE-conjugated anti-His tag antibody was added to the adipocytes under non-permeablizing conditions. PBS was used as a control. **(D)** Binding of SAA1 to the adipocyte cell surface is saturable. Increasing concentrations of His-SAA1 were added to adipocytes for 30 min at 4°C. SAA bound to the cell surface was then detected by flow cytometry under non-permeablizing conditions using a PE-conjugated anti-His tag antibody. Means±SEM from at least n=3 are plotted. $^{**}P<0.01$ by Student's t test. **(E)** ^{3}H-retinol (358 nM) was added to adipocytes with or without pre-incubation with SAA1 (1.07 μM). After incubating for 3 hours at 37°C, the ^{3}H-retinol in the cell pellet was measured and normalized by cell number as a readout of retinol uptake.

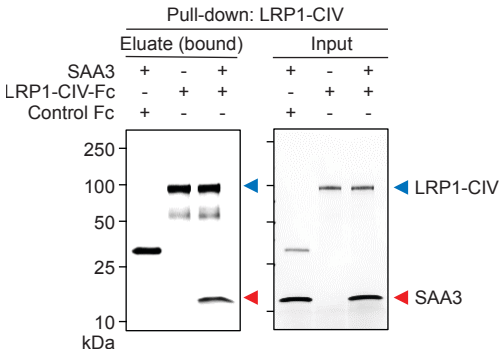

Fig. S2. Mouse SAA3 binds to LRP1-CIV. Binding of mouse SAA3 to LRP1 ligand binding cluster CIV (LRP1-CIV) was tested by pull-down assay. Fc-tagged LRP1-CIV and Fc protein (negative control) were incubated with purified recombinant SAA3. Input proteins are shown (right). Protein G magnetic beads were used to capture Fc-tagged LRP1-CIV or control Fc proteins in the eluate (left).

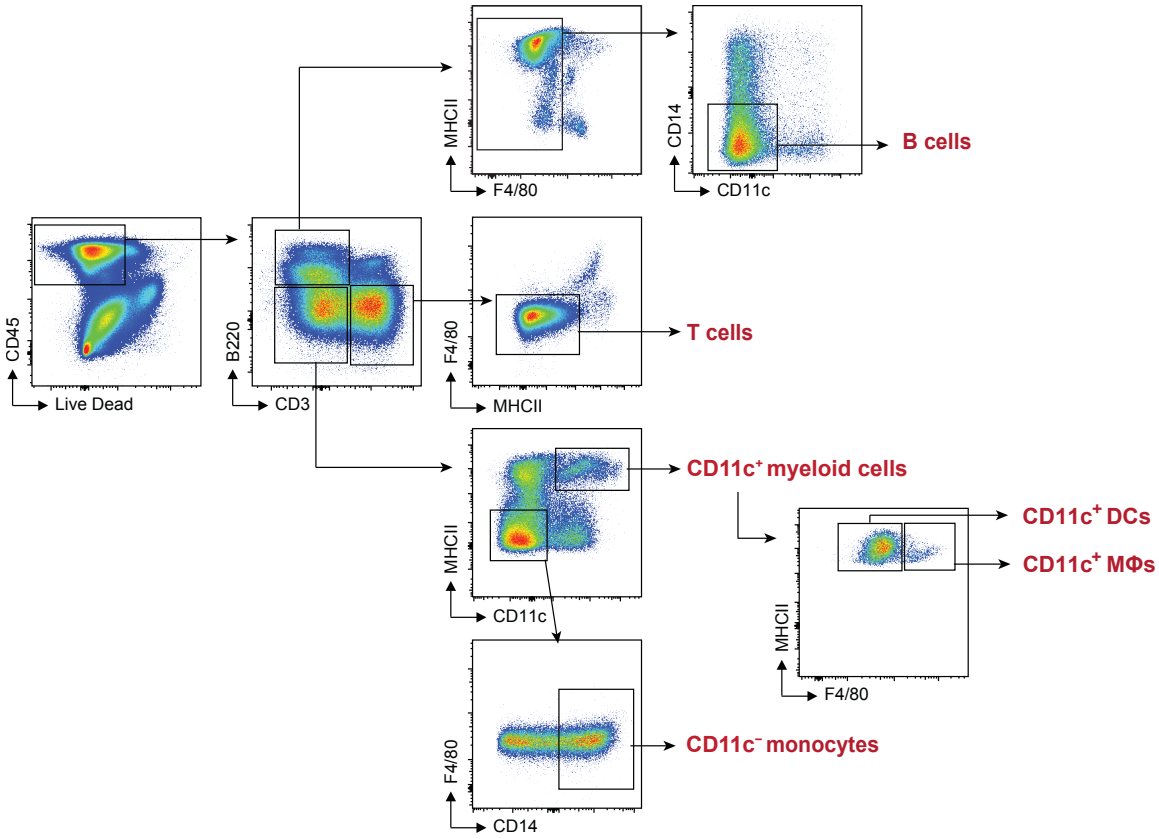

Fig. S3. Flow cytometry gating strategy for assessing LRP1 expression. Small intestinal lamina propria cells were isolated and analyzed by flow cytometry. B cells (live $CD45^+B220^+CD3^-CD14^-F4/80^-CD11c^-$), T cells (live $CD45^+CD3^+B220^-F4/80^-MHCII^-$), $CD11c^-$ monocytes (live $CD45^+CD14^+CD3^-B220^-MHCII^-CD11c^-$), and $CD11c^+$ myeloid cells (live $CD45^+CD11c^+MHCII^+CD3^-B220^-$) were gated as shown. $CD11c^+$ myeloid cells were further gated into DCs (live $CD45^+CD11c^+MHCII^+F4/80^-CD3^-B220^-$) and macrophages (live $CD45^+CD11c^+MHCII^+F4/80^+CD3^-B220^-$). Representative plots are presented and LRP1 expression on each cell population is shown in Fig. 3F and G.

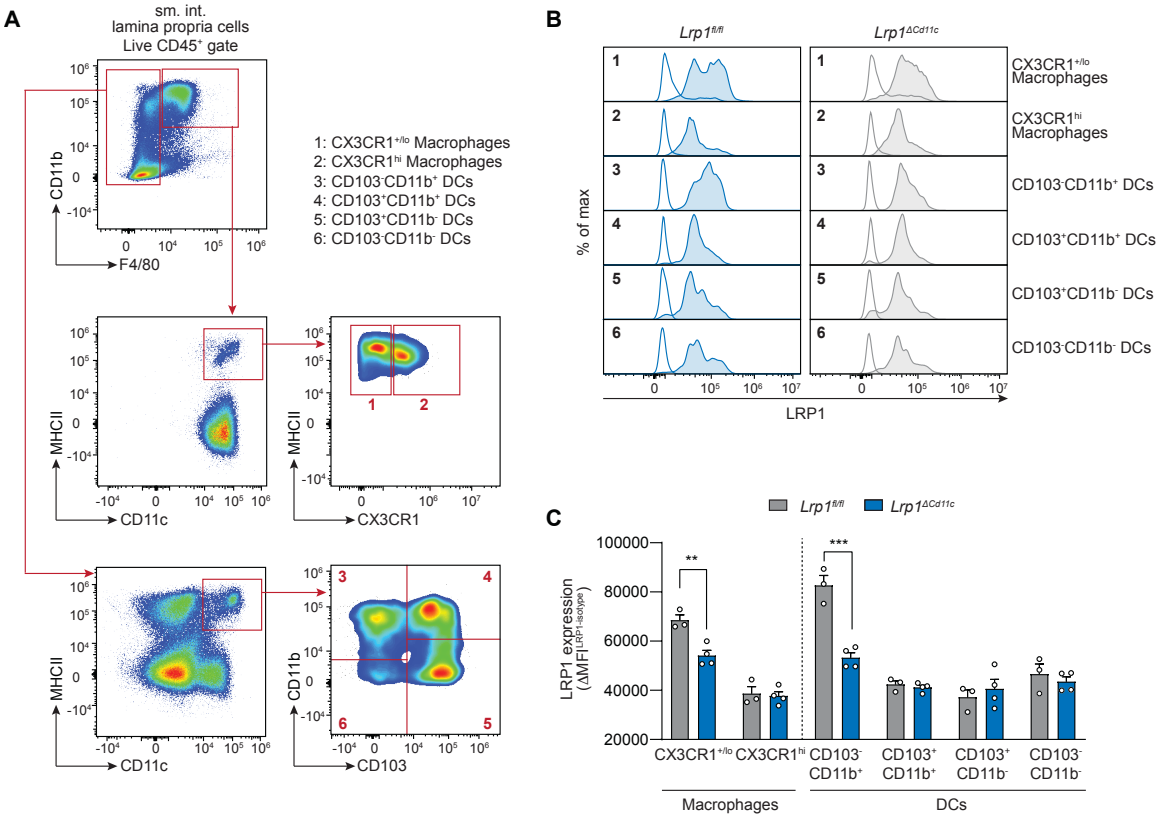

Fig. S4. Expression of LRP1 by CD11c$^+$ myeloid cell subpopulations in mouse small intestine. Small intestinal lamina propria cells were isolated and analyzed by flow cytometry. **(A)** Gating strategy for assessing LRP1 expression. Macrophages (live CD45$^+$F4/80$^+$CD11b$^+$CD11c$^+$MHCII$^+$) were further gated by their expression of CX3CR1. DCs (live CD45$^+$F4/80$^-$CD11c$^+$MHCII$^+$) were further gated by their expression of CD103 and CD11b. Representative plots are presented. **(B)** Representative histograms showing LRP1 expression on each cell population are shown. Empty histograms are from isotype controls. **(C)** LRP1 expression (ΔMFI) is shown as the difference in MFI between isotype-matched control and anti-LRP1 antibody staining (MFI^{LRP1}–MFI^{isotype}). Means±SEM are plotted. $^{**}P<0.01$; $^{***}P<0.001$; by Student's *t* test.

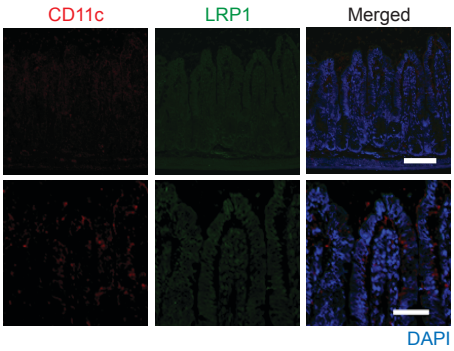

Fig. S5. Immunofluorescence controls for Fig. 3G. Immunofluorescence analysis of mouse ileum with isotype control antibodies (rabbit IgG and Armenian hamster IgG). Cy3-conjugated donkey anti-rabbit IgG and AlexaFluor647-conjugated goat anti-Armenian hamster IgG were used for secondary antibodies. Nuclei are stained with DAPI. Scale bar is 100 μm for the upper panel and 50 μm for the lower panel.

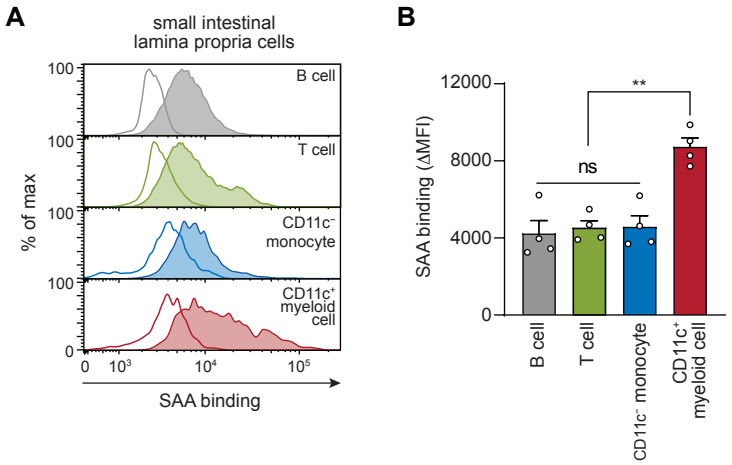

Fig. S6. Binding of SAA–retinol complexes to small intestinal immune cells. Small intestinal lamina propria cells were isolated and incubated with His-SAA1–retinol complexes at 4°C. Binding of His-SAA1–retinol complexes to cells was then analyzed by flow cytometry. B cells ($CD45^+B220^+CD3^-CD14^-CD11c^-$), T cells ($CD45^+CD3^+B220^-CD14^-MHCII^-$), $CD11c^-$ monocytes ($CD45^+CD14^+CD3^-B220^-MHCII^-CD11c^-$), and $CD11c^+$ myeloid cells ($CD45^+CD11c^+MHCII^+CD3^-B220^-$) were gated. **(A)** Representative histograms are shown. Empty histograms are controls in which PBS was added instead of SAA1, and filled histograms are samples with SAA1 added. All samples including controls were stained with a PE-conjugated anti-His antibody. **(B)** SAA1 binding was calculated as ΔMFI (median fluorescence intensity) of SAA1 ($MFI^{SAA1}–MFI^{PBS}$). Means±SEM from n=4 mice are plotted. **P<0.01 by Student's t test.

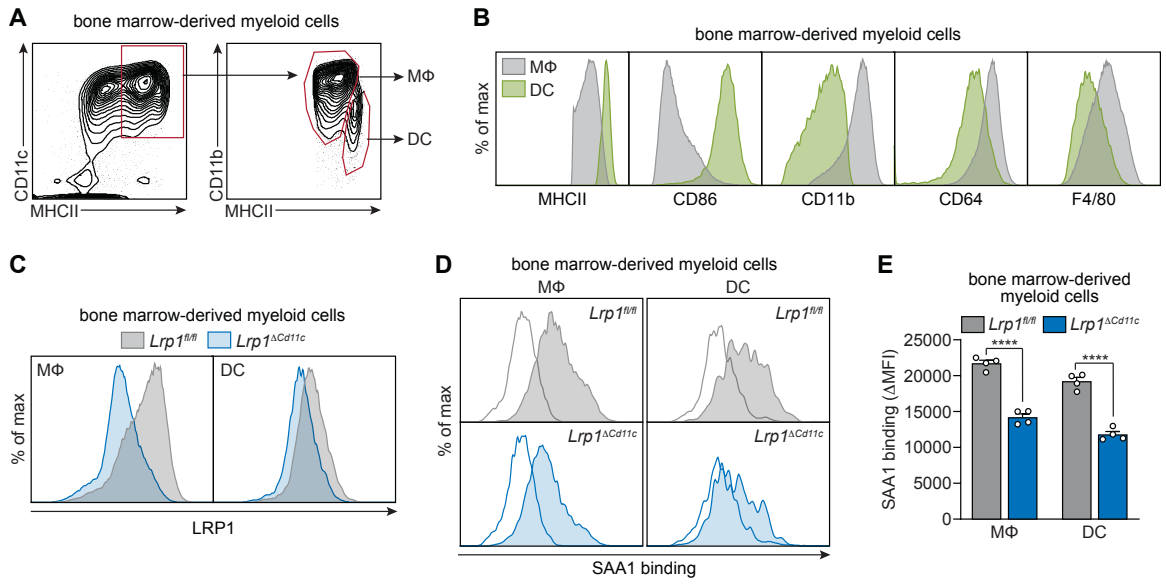

Fig. S7. Analysis of dendritic cells and macrophages for LRP1 expression and SAA1 binding. Bone marrow-derived cells from *Lrp1*$^{fl/fl}$ and *Lrp1*$^{\Delta Cd11c}$ mice were cultured with GM-CSF (granulocyte-macrophage colony-stimulating factor) and CD11c^{+} bone marrow-derived myeloid cells were isolated by CD11c magnetic bead sorting and analyzed by flow cytometry. **(A)** Gating strategy for identification of macrophages (MΦ) (CD11c^{+}MHCII^{+}CD11b^{hi}) and dendritic cells (DC) (CD11c^{+}MHCII^{hi}CD11b$^{+/int}$) are shown. **(B)** Expression of MHCII, CD86, CD11b, CD64, F4/80 on macrophages and dendritic cells were analyzed. Macrophages are MHCII^{+}CD86^{-}CD11b^{hi}CD64^{+}F4/80^{+}, and dendritic cells are MHCII^{hi}CD86^{+}CD11b$^{+/int}$CD64^{-}F4/80^{-}. **(C)** Expression of LRP1 on macrophages and DC from *Lrp1*$^{fl/fl}$ and *Lrp1*$^{\Delta Cd11c}$ mice. **(D and E)** SAA1 binding to macrophages and DC from *Lrp1*$^{fl/fl}$ and *Lrp1*$^{\Delta Cd11c}$ mice. His-SAA1–retinol complexes were added to bone marrow-derived myeloid cells at 4°C to allow binding of SAA1 to the cell surface. Cells were then washed, fixed, and stained with antibodies. **(D)** Representative histograms are shown. Empty histograms are controls in which PBS was added instead of SAA1, and filled histograms are samples with SAA1 added. All samples including controls were stained with a PE-conjugated anti-His antibody. **(E)** SAA1 binding was calculated as ΔMFI (median fluorescence intensity) of SAA1 (MFI^{SAA1}–MFI^{PBS}). Means±SEM from n=4 are plotted. ****P<0.0001 by Student's t test. MΦ, macrophage; DC, dendritic cells.

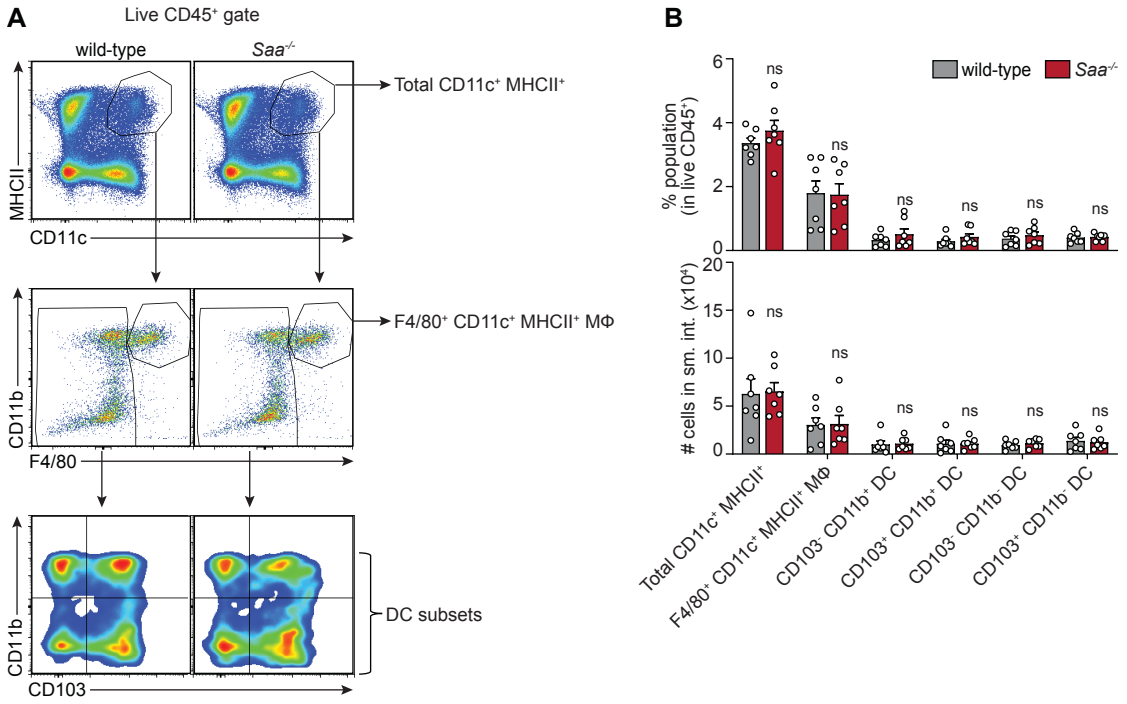

Fig. S8. Characterization of small intestinal CD11c$^+$MHCII$^+$ cells from wild-type and *Saa*$^{-/-}$ mice. Small intestinal lamina propria cells from wild-type and *Saa*$^{-/-}$ mice were analyzed for their CD11c$^+$MHCII$^+$ cell numbers and compositions. **(A)** Representative flow cytometry plots showing gating strategies. **(B)** Percentages among total live CD45$^+$ cells (top) and absolute cell numbers (bottom) of each cell population are shown. Means±SEM are plotted. ns, not significant by Student's *t* test. sm. int., small intestine.

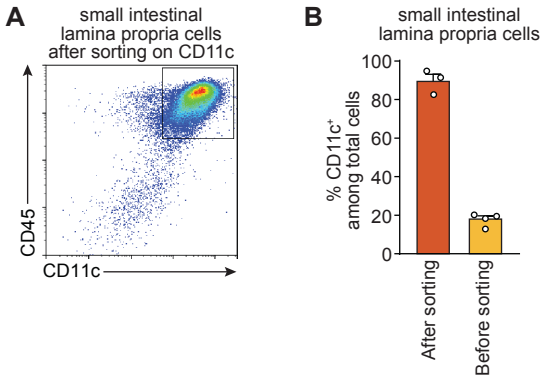

Fig. S9. Magnetic sorting of small intestinal lamina propria CD11c$^+$ cells. Mouse small intestinal lamina propria CD11c$^+$ cells were isolated using anti-CD11c beads. **(A)** A representative flow cytometry plot of cells after bead isolation is shown. **(B)** Percentage of CD11c$^+$ cells among total cells before and after sorting. Means±SEM are plotted.

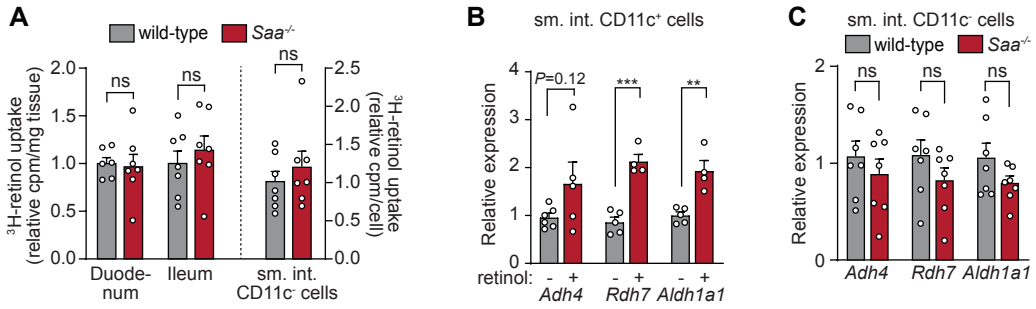

Fig. S10. Retinol uptake in tissues and cells from wild-type and *Saa*$^{-/-}$ mice. (A) ^{3}H-retinol was fed to wild-type and *Saa*$^{-/-}$ mice. Following sacrifice, the duodenum (proximal small intestine) and ileum (distal small intestine) were flushed to remove the fecal contents, and lamina propria cells were recovered and separated into CD11c^{+} and CD11c^{-} cell populations using CD11c magnetic beads. The CD11c^{+} cells were used in experiments depicted in Fig. 5, A and B, and the negatively selected CD11c^{-} cells were analyzed in the experiments depicted in this figure. ^{3}H-retinol cpm were normalized to tissue weight (for duodenum and ileum) or to cell number (for CD11c^{-} cells). **(B)** Immune cells were recovered from the small intestinal lamina propria of *Saa*$^{-/-}$ mice and the CD11c^{+} cells were isolated by magnetic bead sorting. CD11c^{+} cells were incubated with or without 100 μM retinol for 2 hours in a 5% CO_2 incubator at 37°C. Transcript abundances were normalized to *Gapdh* transcript abundance and expressed relative to no retinol controls. **(C)** Small intestinal lamina propria CD11c^{-} cells were used for qPCR analysis of transcripts encoding proteins involved in retinol conversion to retinoic acid. Transcript abundances were normalized to *Gapdh* transcript abundance and expressed relative to wild-type transcript abundances. sm. int., small intestine. Means±SEM from at least n=3 mice are plotted. **P<0.01; ***P<0.001; ns, not significant by Student's t test.

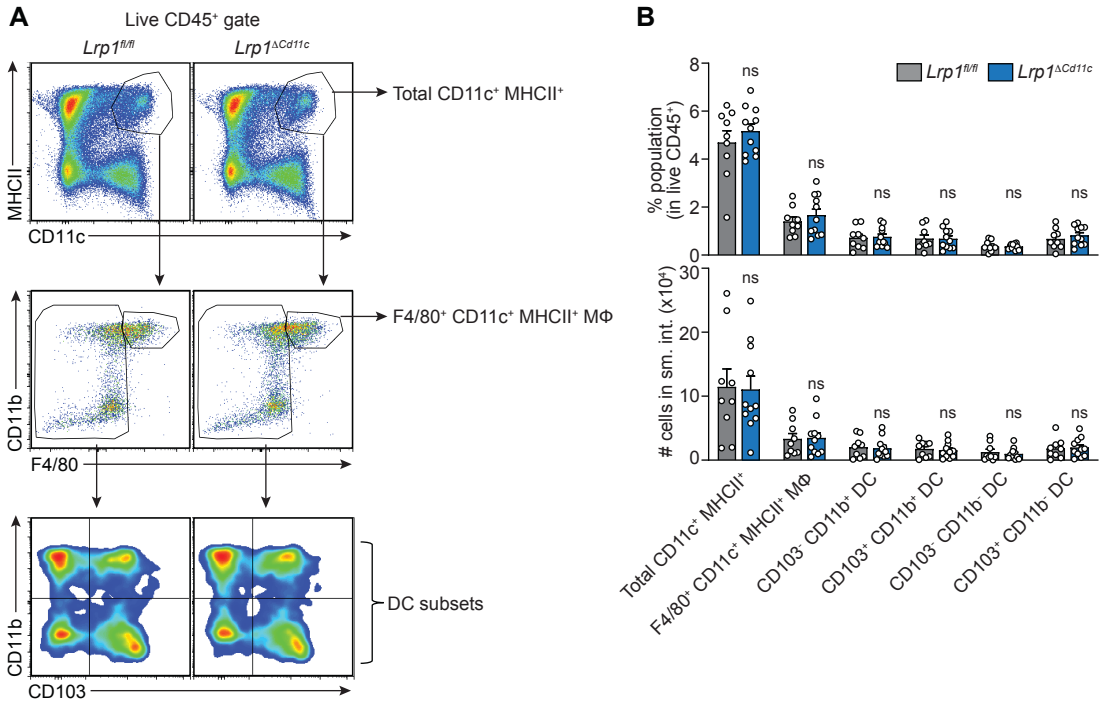

Fig. S11. Characterization of small intestinal CD11c^{+}MHCII^{+} cells from *Lrp1$^{fl/fl}$* and *Lrp1$^{\Delta Cd11c}$* mice. Small intestinal lamina propria cells from *Lrp1$^{fl/fl}$* and *Lrp1$^{\Delta Cd11c}$* mice were analyzed for CD11c^{+}MHCII^{+} cell numbers and composition. **(A)** Representative flow cytometry plots showing gating strategies. **(B)** Percentages among total live CD45^{+} cells (top) and absolute cell numbers (bottom) of each cell population are shown. Means±SEM are plotted. ns, not significant by Student's *t* test. sm. int., small intestine.

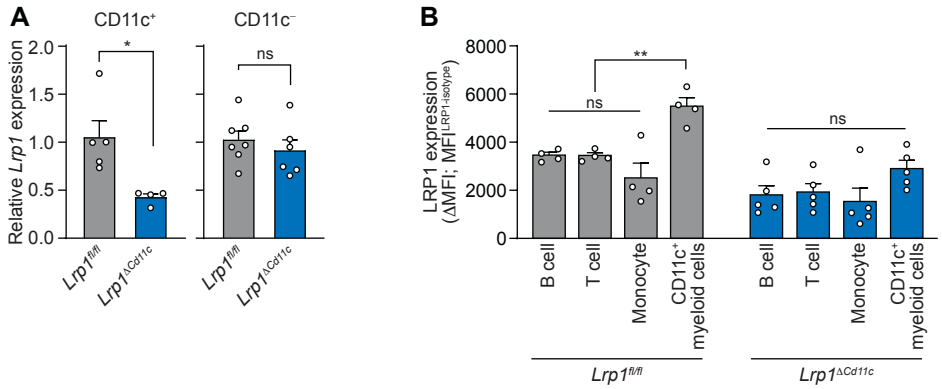

Fig. S12. LRP1 expression in intestinal CD11c$^+$ cells from *Lrp1$^{fl/fl}$* and *Lrp1$^{\Delta Cd11c}$* mice. (A) qPCR analysis of *Lrp1* expression in small intestinal lamina propria CD11c$^+$ and CD11c$^-$ cells from *Lrp1$^{fl/fl}$* and *Lrp1$^{\Delta Cd11c}$* mice. **(B)** Flow cytometry analysis of LRP1 expression on B cells, T cells, monocytes, and CD11c$^+$ myeloid cells from the small intestinal lamina propria of *Lrp1$^{fl/fl}$* and *Lrp1$^{\Delta Cd11c}$* mice. LRP1 expression was determined by subtracting isotype-matched control MFI from LRP1 MFI of each cell population (MFI^{LRP1}–MFI^{isotype}). Means±SEM are plotted. **P*<0.05; ***P*<0.01; ns, not significant as determined by Student's *t* test. MFI, median fluorescence intensity.

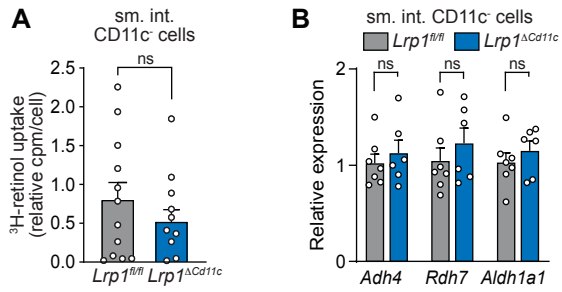

Fig. S13. Retinol quantification in tissues and cells from *Lrp1*$^{fl/fl}$ and *Lrp1*$^{\Delta Cd11c}$ mice. **(A)** ^{3}H-retinol was fed to *Lrp1*$^{fl/fl}$ and *Lrp1*$^{\Delta Cd11c}$ mice. Small intestinal lamina propria cells were recovered and processed with magnetic bead isolation using anti-CD11c beads. CD11c^{+} cells were analyzed in Fig. 5, E and F, and CD11c^{-} cells were analyzed here. ^{3}H-retinol cpm were normalized to cell number. **(B)** Small intestinal lamina propria CD11c^{-} cells from CD11c magnetic sorting were used for qPCR analysis of transcripts encoding proteins involved in retinol conversion to retinoic acid. Transcript abundances were normalized to *Gapdh* transcript abundance and expressed relative to *Lrp1*$^{fl/fl}$ transcript abundances. Means±SEM are plotted. ns, not significant by Student's *t* test.

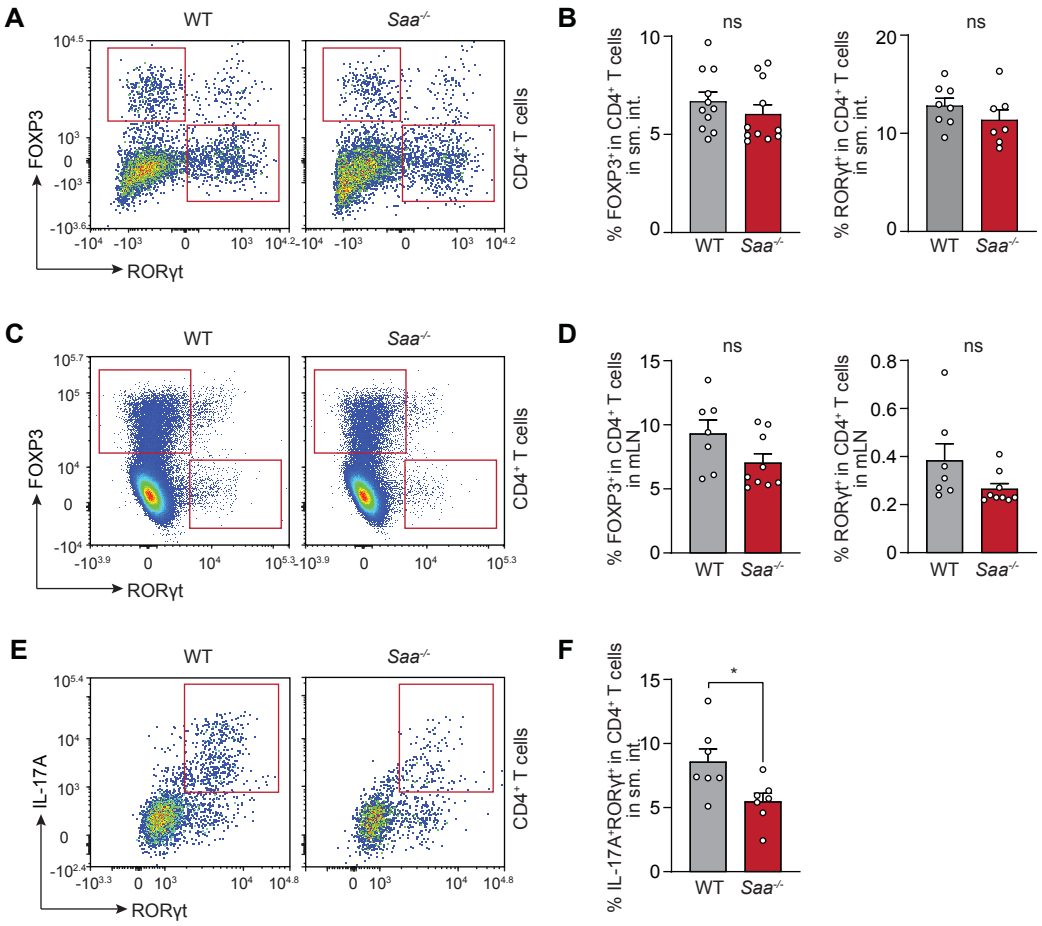

Fig. S14. T_{reg} and T_H17 cell frequencies in the small intestines and mesenteric lymph nodes of wild-type and *Saa*$^{-/-}$ mice. (A and C) Representative flow plots of T cells ($CD45^+CD3^+CD4^+$) expressing FOXP3 and RORγt, which mark T_{reg} and T_H17 cells, respectively. Cells were isolated from the small intestinal lamina propria (A) and mesenteric lymph nodes (C) of wild-type and *Saa*$^{-/-}$ mice and stained with antibodies against the indicated T cell markers. **(B)** Quantification of T_{reg} and T_H17 cell frequencies in A. **(D)** Quantification of T_{reg} and T_H17 frequencies in C. **(E and F)** $IL\text{-}17^+ROR\gamma t^+$ T_H17 cells from small intestinal lamina propria cells of wild-type and *Saa*$^{-/-}$ mice. Representative flow plots of T cells ($CD45^+CD3^+CD4^+$) expressing RORγt and IL-17A (E) and quantification (F) are shown. Means±SEM are plotted. *P<0.05; ns, not significant as determined by Student's t test. sm. int., small intestine. mLN, mesenteric lymph nodes.

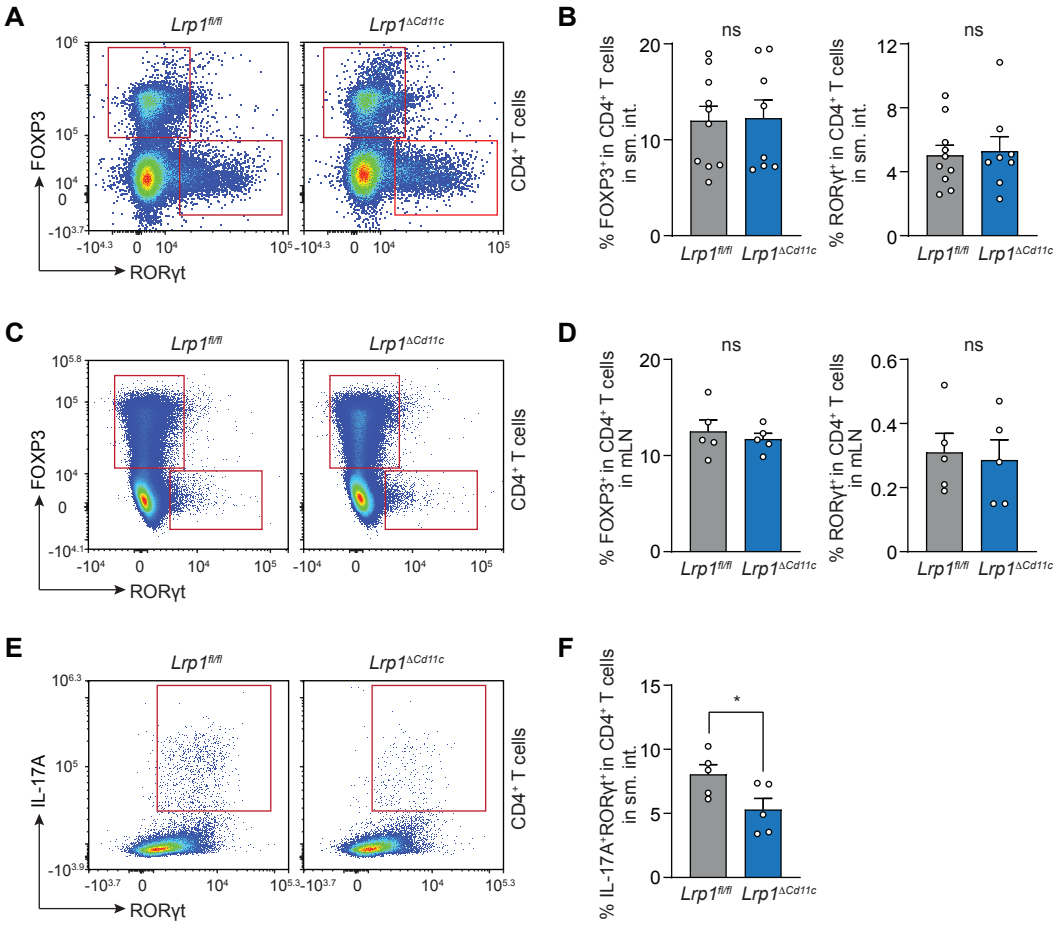

Fig. S15. T_{reg} and T_H17 cell frequencies in the small intestines and mesenteric lymph nodes of *Lrp1*$^{fl/fl}$ and *Lrp1*$^{\Delta Cd11c}$ mice. (A and C) Representative flow plots of T cells ($CD45^+CD3^+CD4^+$) expressing FOXP3 and RORγt, which marks T_{reg} and T_H17 cells, respectively. Cells were isolated from the lamina propria of small intestines (A) and mesenteric lymph nodes (C) of *Lrp1*$^{fl/fl}$ and *Lrp1*$^{\Delta Cd11c}$ mice and stained with antibodies against the indicated T cell markers. **(B)** Quantification of T_{reg} and T_H17 frequencies in A. **(D)** Quantification of T_{reg} and T_H17 frequencies in C. **(E and F)** IL-17^+RORγt^+ T_H17 cells from small intestinal lamina propria cells of *Lrp1*$^{fl/fl}$ and *Lrp1*$^{\Delta Cd11c}$ mice. Representative flow plots of T cells ($CD45^+CD3^+CD4^+$) expressing RORγt and IL-17A (E) and quantification (F) are shown. Means±SEM are plotted. **P*<0.05; ns, not significant as determined by Student's *t* test. sm. int., small intestine. mLN, mesenteric lymph nodes.

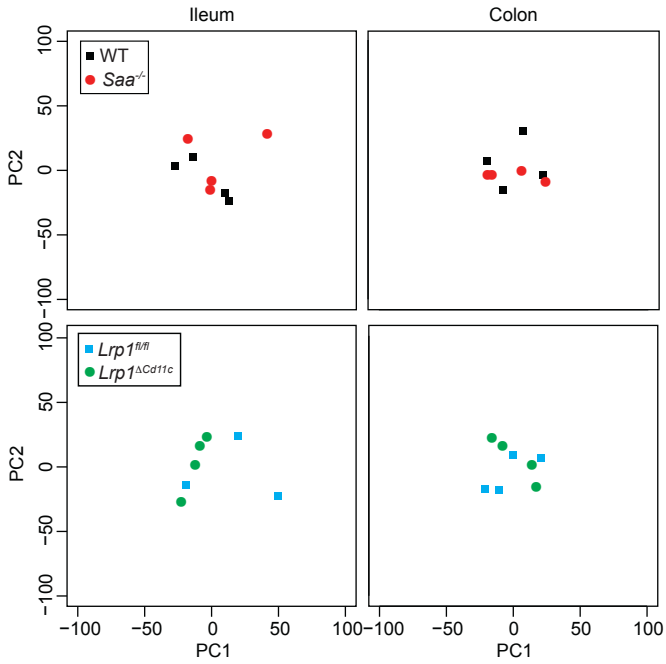

Fig. S16. Intestinal microbiota analysis. Principal coordinate analysis of 16*S* rRNA sequencing of mouse intestinal contents. Ileal and cecal contents from wild-type and *Saa*$^{-/-}$ mice, and *Lrp1*$^{fl/fl}$ and *Lrp1*$^{\Delta Cd11c}$ mice, were analyzed. The mice were littermates of heterozygous crosses that remained cohoused. Each dot represents one mouse.

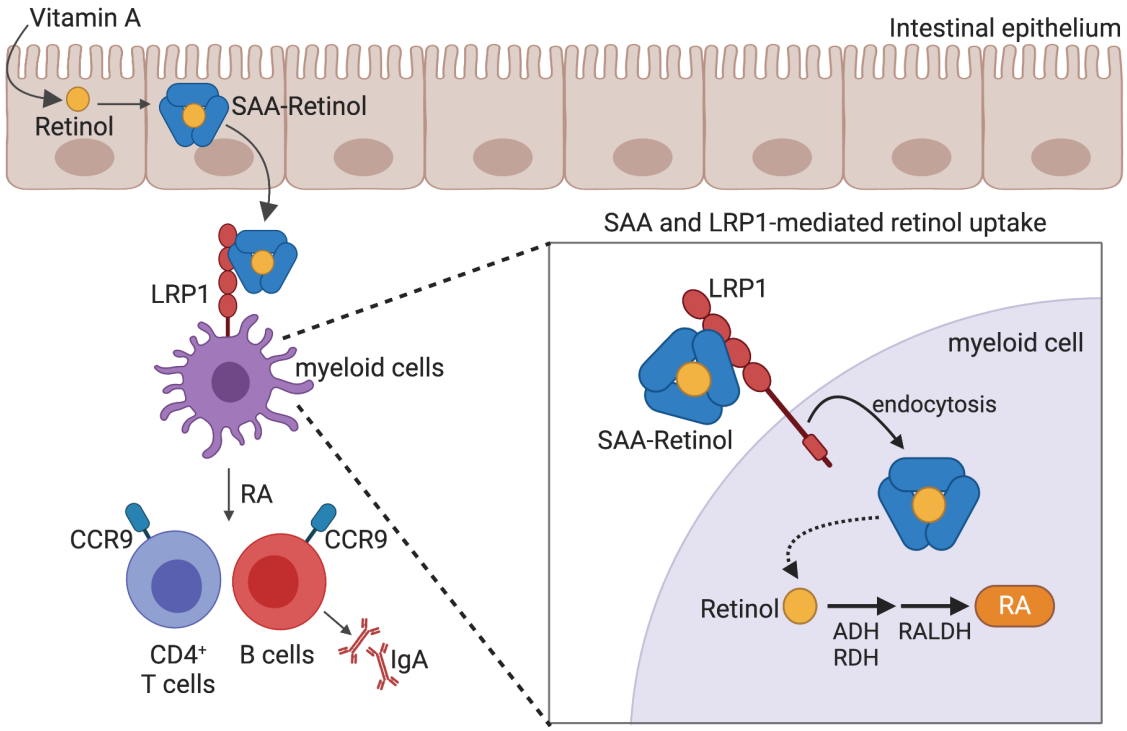

Fig. S17. SAA delivers retinol to myeloid cells by binding to LRP1 and thus promotes adaptive immunity in the intestine. SAA delivers retinol to intestinal CD11c$^+$ myeloid cells by binding to LRP1. LRP1 facilitates endocytosis of SAA–retinol complexes, and the retinol is converted to retinoic acid (RA) through a two-step enzymatic reaction. Myeloid cell RA promotes vitamin A-dependent intestinal adaptive immune responses. These include the induction of intestinal homing receptors, such as CCR9, on CD4$^+$ T cells and B cells, and IgA production by B cells. Illustration was created in BioRender (BioRender.com).

Table S1. Mass spectrometry analysis of protein complexes from Fig. 1B

Protein	Length (AA)	Mw (Da)	% Coverage	PSMs*	Peptide Seqs†	MIC Sin§
His-tagged SAA1	124	14075.5	99.20	1080	21	3.06E-03
LDL receptor-related protein 1	4545	505761.0	29.60	543	111	2.38E-06

*PSMs (Peptide Spectrum Matches): Number of spectra assigned to peptides that contributed to the inference of the protein.
†Peptide Seqs: Number of different unique peptide sequences, or modified variants of sequences that were identified for the protein.
§MIC Sin: The normalized Spectral Index statistic for the protein (quantitative, approximate)

Table S2. TaqMan probes used for qPCR

Gene name	Description	Assay ID
Gapdh	Glyceraldehyde-3-phosphate dehydrogenase	Mm99999915_g1
Saa1	Serum amyloid A1	Mm00656927_g1
Rbp4	Retinol binding protein 4	Mm00803264_g1
Lrp1	LDL receptor-related protein 1	Mm00464608_m1
Lrp1	LDL receptor-related protein 1 (Exon1; used in fig. S12A)	Mm01160430_m1
Stra6	Stimulated by retinoic acid gene 6	Mm00486457_m1
Rbpr2	RBP receptor 2; STRA6-like	Mm01345313_m1
Adh4	Alcohol dehydrogenase 4	Mm00478838_m1
Rdh7	Retinol dehydrogenase 7	Mm00489956_g1
Aldh1a1	Aldehyde dehydrogenase family 1, subfamily A1	Mm00657317_m1

Table S3. Antibodies used for flow cytometry

Specificity	Clone	Isotype	Fluoro-chrome	Supplier	Catalog number	Final concentration
LRP1	EPR3724	Rabbit IgG	AlexaFluor 488	Abcam	ab195567	0.01 µg/µl
CD19	1D3	Rat IgG2a	FITC	Invitrogen	11-0193-82	0.01 µg/µl
IL-17A	TC11-18H10.1	Rat IgG1κ	FITC	Biolegend	506907	0.025 µg/µl
IgA	11-44-2	Rat IgG1	PE	Invitrogen	12-5994-81	0.01 µg/µl
CCR9	CW-1.2	Mouse IgG2a	PE	Invitrogen	12-1991-80	0.005 µg/µl
6xHistidine	AD1.1.10	Mouse IgG1	PE	R&D Systems	IC050P	1:100 (*v*/*v*)
CD11b	M1/70	Rat IgG2b	PE	Biolegend	101208	0.0025 µg/µl
CD4	RM4-5	Rat IgG2a	PE	Biolegend	100512	0.0025 µg/µl
B220	RA3-6B2	Rat IgG2a	PE-Cyanine5	Invitrogen	15-0452-82	0.0025 µg/µl
CD11c	N418	Armenian Hamster IgG	PE-Cyanine5	Invitrogen	15-0114-82	0.005 µg/µl
Foxp3	FJK-16s	Rat IgG2a	PE-Cyanine5	Invitrogen	15-5773-80	0.01 µg/µl
CD4	RM4-5	Rat IgG2a	PE-Cyanine7	Biolegend	100528	0.002 µg/µl
CD103	2E7	Armenian Hamster IgG	PE-Cyanine7	Biolegend	121426	0.002 µg/µl
MHCII	M5/114.15.2	Rat IgG2b	PE-Cyanine7	Biolegend	107630	0.0006 µg/µl
CD14	Sa2-8	Rat IgG2a	PerCP-eFluor 710	Invitrogen	46-0141-82	0.005 µg/µl
CD8a	53-6.7	Rat IgG2a	APC	Invitrogen	17-0081-82	0.004 µg/µl
MHCII	M5/114.15.2	Rat IgG2b	APC	Invitrogen	17-5321-82	0.0003 µg/µl
CD86	GL-1	Rat IgG2a	APC	Biolegend	139323	0.0025 µg/µl
CD3	17A2	Rat IgG2b	APC	R&D Systems	FAB4841A-100	10 µl/10^6 cells
RORγt	AFKJS-9	Rat IgG2a	APC	Invitrogen	17-6988-82	0.01 µg/µl
CD45	30-F11	Rat IgG2b	Brilliant violet 421	Biolegend	103134	0.002 µg/µl
CD11c	N418	Armenian Hamster IgG	Brilliant violet 421	Biolegend	117343	0.0025 µg/µl
F4/80	BM8	Rat IgG2a	Brilliant violet 510	Biolegend	123135	0.004 µg/µl
CD64	X54-5/7.1	Mouse IgG1	Brilliant violet 605	Biolegend	139323	0.0024 µg/µl
CD45	30-F11	Rat IgG2b	Brilliant violet 650	Biolegend	103151	0.002 µg/µl
CD8a	53-6.7	Rat IgG2a	Brilliant violet 650	Biolegend	100742	0.0025 µg/µl
CD3	17A2	Rat IgG2b	Brilliant violet 711	Biolegend	100241	0.004 µg/µl
F4/80	T45-2342	Rat IgG2a	Brilliant violet 711	BD Biosciences	565612	0.006 µg/µl
CX3CR1	SA011F11	Mouse IgG2a	Brilliant violet 785	Biolegend	149029	0.00125 µg/µl